

Chaos and Complexity in Quantum Mechanics

Tibra Ali^{(a) 1}, Arpan Bhattacharyya^{(b) 2}, S. Shajidul Haque^{(c)3},
Eugene H. Kim^{(c)4}, Nathan Moynihan^{(d)5}, Jeff Murugan^{(d)6}

^(a) *Perimeter Institute,*

31 Caroline Street North

Waterloo, Ontario, Canada, N2L 2Y5

^(b) *Center for Gravitational Physics,*

Yukawa Institute for Theoretical Physics (YITP), Kyoto University,

Kitashirakawa Oiwakecho, Sakyo-ku, Kyoto 606-8502, Japan

^(c) *Department of Physics, University of Windsor,*

401 Sunset Avenue

Windsor, Ontario, Canada, N9B 3P4

^(d) *The Laboratory for Quantum Gravity & Strings,*

Department of Mathematics & Applied Mathematics,

University of Cape Town,

Private Bag, Rondebosch, 7701, South Africa

Abstract

We propose a new diagnostic for quantum chaos. We show that time evolution of complexity for a particular type of target state can provide equivalent information about the classical Lyapunov exponent and scrambling time as out-of-time-order correlators. Moreover, for systems that can be switched from a regular to unstable (chaotic) regime by a tuning of the coupling constant of the interaction Hamiltonian, we find that the complexity defines a new time scale. We interpret this time scale as recording when the system makes the transition from regular to chaotic behaviour.

¹tali@perimeterinstitute.ca

²bhattacharyya.arpan@yahoo.com

³shajid.haque@uwindsor.ca

⁴ehkim@uwindsor.ca

⁵nathanmoynihan@gmail.com

⁶jeff.murugan@uct.ac.za

1 Introduction

Quantum chaos is intrinsically difficult to characterize. Consequently, a precise definition of quantum chaos in many-body systems remains elusive and our understanding of the dynamics of quantum chaotic systems is still inadequate. This lack of understanding is at the heart of a number of open questions in theoretical physics such as thermalization and transport in quantum many-body systems, and black hole information loss. It has also precipitated the renewed interest in quantum chaos from various branches of physics from condensed matter physics to quantum gravity [1].

Chaotic classical systems on the other hand are characterised by their *sensitive dependence on initial conditions* — two copies of such a system, prepared in nearly identical initial states (namely, two distinct points in phase space, separated by a very small distance), will evolve over time into widely separated configurations. More precisely, the distance between the two points in phase space grows as $\exp(\lambda_L t)$, where λ_L is the system’s largest Lyapunov exponent [2]. This does not happen in quantum mechanics — two nearly identical states, *i.e.* states with a large initial overlap, remain nearly identical for all time (as their overlap is constant under unitary evolution). It has been argued [3, 4] that a quantum analog of “sensitive dependence on initial conditions” is to consider evolving identical states with slightly different Hamiltonians, \hat{H} and $\hat{H} + \delta\hat{H}$. If \hat{H} is the quantization of a (classically) chaotic Hamiltonian, the states will evolve into two different states whose inner product decays exponentially in time.

Traditionally, chaos in quantum systems has been identified by comparison with results from random matrix theory (RMT)[5]. Recently however, other diagnostics have been proposed to probe chaotic quantum systems [6, 7, 8]. One such diagnostic is out-of-time-order correlators (OTOCs) [9, 10] from which both the (classical) Lyapunov exponent as well as the scrambling time [11, 12, 13] may be extracted. However, recent work in mass-deformed SYK models [14] have revealed some tension between the OTOC and RMT diagnostics that arise, in part, through the nature of the probes. The OTOC captures early-time quantum mechanical features of the system while RMT diagnostics typically capture late-time statistical features. Evidently, a deeper understanding of probes of quantum chaos is required. In this light, it is interesting therefore to ask whether one can characterize chaos in quantum systems using quantum information-theoretic measures⁷. In this work, we propose a new diagnostic/probe of quantum chaos using the notion of *circuit complexity* [15, 16, 17, 18, 19, 20, 21, 22, 23, 24, 25, 26, 27], adopting Nielsen’s geometric approach [28, 29, 30]. More specifically, we study the circuit complexity of a particular target state obtained from a reference state by performing a forward evolution followed by a backward evolution with slightly different Hamiltonians. Then we demonstrate how this enables one to probe/characterize chaotic quantum systems, giving information beyond what is contained in the OTOC. Note that instead of using the complexity for a target state that is forward and then backward evolved from a reference state as mentioned above, one can as well study the complexity of a different circuit where both the target and reference states are obtained from time evolution (once) by applying slightly different Hamiltonians from some common state. For circuit complexity from the correlation matrix method that we will be using in this paper, the authors of [22] concretely showed that the time evolution

⁷Some progress in this direction was made in [31, 32, 33, 34, 35, 36, 37].

of complexity in these two scenarios is identical.

To establish our testing method, we consider a simple, exactly solvable system — the inverted oscillator, described by the Hamiltonian $H = p^2/2 - \omega^2 x^2/2$ [38] — which captures the exponential sensitivity to initial conditions exhibited by chaotic systems [39]. Classically, the inverted oscillator has an unstable fixed point at $(x = 0, p = 0)$; a particle accelerates exponentially away from the fixed point when perturbed. Though the phase-space volume of the inverted oscillator is unbounded, our results are relevant to systems with a bounded phase space in that such a system would be described by an inverted oscillator up to a certain time. The two systems produce the same results over the time of interest (but would not be analytically solvable beyond that time). In what follows, we include the analysis for a regular oscillator as a reference for what arises in a non-chaotic system and explore also a many-body system (quantum field theory) where the inverted oscillator appears. It is worth noting the inverted quantum oscillator is not just a toy model; it has been realized experimentally [40] and has even played a role in mathematics, in attacking the Riemann hypothesis [41]. It also provides important insights into the bound of the Lyapunov exponents [42].

The rest of the paper is organized as follows. In Section 2, we present the model and states considered in this work. In Section 3, we review the ideas behind circuit complexity, and compute the circuit complexity for our system. Sections 4 and 5 demonstrate how quantum chaos can be detected and quantified using circuit complexity while Section 6 discusses the OTOC and its relation to the results obtained from the circuit complexity. In Section 7, we discuss a many-body system (quantum field theory) where the inverted oscillator arises. Finally, we summarize and present concluding remarks in Section 8.

2 The Model

We are interested in comparing the complexity of a regular system with that of an unstable/chaotic system. To that end, we consider the Hamiltonian

$$H = \frac{1}{2}p^2 + \frac{\Omega^2}{2}x^2 \quad \text{where} \quad \Omega^2 = m^2 - \lambda. \quad (1)$$

For $\lambda < m^2$, equation (1) describes a simple harmonic oscillator; for $\lambda > m^2$, we have an inverted oscillator. The $\lambda = m^2$ case, of course describes a free particle. Our inverted oscillator model can be understood as a short-time approximation for unstable/chaotic systems. In particular, this model captures the exponential sensitivity to initial conditions exhibited by chaotic systems. Let's start with the following state at $t = 0$,

$$\psi(x, t = 0) = \mathcal{N}(t = 0) \exp\left(-\frac{\omega_r x^2}{2}\right), \quad (2)$$

where

$$\omega_r = m. \quad (3)$$

Evolving this state in time by the Hamiltonian (1) produces [43]

$$\psi(x, t) = \mathcal{N}(t) \exp\left(-\frac{\omega(t) x^2}{2}\right), \quad (4)$$

where $\mathcal{N}(t)$ is the normalization factor and

$$\omega(t) = \Omega \left(\frac{\Omega - i \omega_r \cot(\Omega t)}{\omega_r - i \Omega \cot(\Omega t)} \right). \quad (5)$$

We will be computing the complexity for this kind of time evolved state (4) with respect to (2) and

$$\omega(t=0) = \omega_r. \quad (6)$$

3 Complexity from the Covariance Matrix

We will start this section with a quick review of circuit complexity and then conclude with a computation of the circuit complexity for a single oscillator. For circuit complexity we will use the covariance matrix method. Note that a similar analysis can be done for circuit complexity from the full wave function.

3.1 Review of Circuit Complexity

Here we will briefly sketch the outline of the computation of circuit complexity. Details of this can be found in [15, 17]. We will highlight only the key formulae and interested readers are referred to [15, 17] and citations thereof. The problem is simple enough to state; given a set of elementary gates and a reference state, we want to build the most efficient circuit that starts at the reference state and terminates at a specified target state. Formally,

$$|\psi_{\tau=1}\rangle = \tilde{U}(\tau=1)|\psi_{\tau=0}\rangle, \quad (7)$$

where

$$\tilde{U}(\tau) = \overleftarrow{\mathcal{P}} \exp(i \int_0^\tau d\tau H(\tau)), \quad (8)$$

is the unitary operator representing the quantum circuit, which takes the reference state $|\psi_{\tau=0}\rangle$ to the target state $|\psi_{\tau=1}\rangle$. τ parametrizes a path in the space of the unitaries and given a particular basis (elementary gates) M_I ,

$$H(\tau) = Y^I(\tau) M_I.$$

In this context, the coefficients $\{Y^I(\tau)\}$ are referred to as ‘control functions’. The path ordering in (8) is necessary as all the M_I ’s do not necessarily commute with each other.

Now, since the states under consideration (2) and (4) are Gaussian, they can be equivalently described by a *Covariance matrix* as follows

$$G^{ab} = \langle \psi(x, t) | \xi^a \xi^b + \xi^b \xi^a | \psi(x, t) \rangle, \quad (9)$$

where $\xi = \{x, p\}$. This covariance matrix is typically a real symmetric matrix with unit determinant. We will always transform the reference covariance matrix such that [20, 22]

$$\tilde{G}^{\tau=0} = S \cdot G^{\tau=0} \cdot S^T \quad (10)$$

with $\tilde{G}^{\tau=0}$ an identity matrix and S a real symmetric matrix whose transpose is denoted S^T . Similarly, the reference state will transform as

$$\tilde{G}^{\tau=1} = S \cdot G^{\tau=1} \cdot S^T. \quad (11)$$

The unitary $\tilde{U}(\tau)$ acts on this transformed covariance matrix as,

$$\tilde{G}^{\tau=1} = \tilde{U}(\tau) \cdot \tilde{G}^{\tau=0} \cdot \tilde{U}^{-1}(\tau). \quad (12)$$

Next we define suitable *cost function* $\mathcal{F}(\tilde{U}, \dot{\tilde{U}})$ and define [15, 28, 29, 30]

$$\mathcal{C}(\tilde{U}) = \int_0^1 \mathcal{F}(\tilde{U}, \dot{\tilde{U}}) d\tau. \quad (13)$$

Minimizing this cost functional gives us the optimal set of $Y^I(\tau)$, which in turn give us the most efficient circuit by minimizing the circuit depth. There are various possible choices for these functions $\mathcal{F}(\tilde{U}, \dot{\tilde{U}})$. For further details, we refer the reader to the extensive literature in [15, 16, 17, 28, 29, 30]. In this paper, we will choose

$$\mathcal{F}_2(U, Y) = \sqrt{\sum_I (Y^I)^2}. \quad (14)$$

For this choice, one can easily see that, after minimization the $\mathcal{C}(\tilde{U})$ defined in (13) corresponds to the geodesic distance on the manifold of unitaries. Note also that we can reproduce our analysis done in the following sections with other choices of cost functional. We will, however, leave this for future work.

3.2 Circuit Complexity for a Single Oscillator

For our case, the covariance matrix corresponding to target state (4) will take the form,

$$G^{\tau=1} = \begin{pmatrix} \frac{1}{\text{Re}(\omega(t))} & -\frac{\text{Im}(\omega(t))}{\text{Re}(\omega(t))} \\ -\frac{\text{Im}(\omega(t))}{\text{Re}(\omega(t))} & \frac{|\omega(t)|^2}{\text{Re}(\omega(t))} \end{pmatrix}, \quad (15)$$

where $\omega(t)$ is defined in (5). For the reference state (2) it will take the following form,

$$G^{\tau=0} = \begin{pmatrix} \frac{1}{\omega_r} & 0 \\ 0 & \omega_r \end{pmatrix}. \quad (16)$$

Next we change the basis as follows

$$\tilde{G}^{\tau=1} = S \cdot G^{\tau=1} \cdot S^T, \quad \tilde{G}^{\tau=0} = S \cdot G^{\tau=0} \cdot S^T, \quad (17)$$

with

$$S = \begin{pmatrix} \sqrt{\omega_r} & 0 \\ 0 & \frac{1}{\sqrt{\omega_r}} \end{pmatrix}, \quad (18)$$

such that $\tilde{G}^{\tau=0} = I$ is an identity matrix. For the case under study, the reference frequency ω_r is real. We will choose the following three generators,

$$M_{11} \rightarrow \frac{i}{2}(x p + p x), \quad M_{22} \rightarrow \frac{i}{2}x^2, \quad M_{33} \rightarrow \frac{i}{2}p^2. \quad (19)$$

These will serve as our elementary gates and satisfy the $SL(2, R)$ algebra.

$$[M_{11}, M_{22}] = 2 M_{22}, \quad [M_{11}, M_{33}] = -2 M_{33}, \quad [M_{22}, M_{33}] = M_{11}. \quad (20)$$

Next, if we parameterize the $\tilde{U}(\tau)$ as,

$$\tilde{U}(\tau) = \begin{pmatrix} \cos(\mu(\tau)) \cosh(\rho(\tau)) - \sin(\theta(\tau)) \sinh(\rho(\tau)) & -\sin(\mu(\tau)) \cosh(\rho(\tau)) + \cos(\theta(\tau)) \sinh(\rho(\tau)) \\ \sin(\mu(\tau)) \cosh(\rho(\tau)) + \cos(\theta(\tau)) \sinh(\rho(\tau)) & \cos(\mu(\tau)) \cosh(\rho(\tau)) + \sin(\theta(\tau)) \sinh(\rho(\tau)) \end{pmatrix}. \quad (21)$$

and set the boundary conditions as,

$$\tilde{G}^{\tau=1} = \tilde{U}(\tau=1) \cdot \tilde{G}^{\tau=0} \cdot \tilde{U}^{-1}(\tau=1), \quad \tilde{G}^{\tau=0} = \tilde{U}(\tau=0) \cdot \tilde{G}^{\tau=0} \cdot \tilde{U}^{-1}(\tau=0), \quad (22)$$

we find that [22],

$$\{\cosh(2\rho(1)), \tan(\theta(1) + \mu(1))\} = \left\{ \frac{\omega_r^2 + |\omega(t)|^2}{2\omega_r \operatorname{Re}(\omega(t))}, \frac{\omega_r^2 - |\omega(t)|^2}{2\omega_r \operatorname{Im}(\omega(t))} \right\}, \quad \{\rho(0), \theta(0) + \mu(0)\} = \{0, c\}. \quad (23)$$

Here c is an arbitrary constant. For simplicity we choose

$$\mu(\tau=1) = \mu(\tau=0) = 0, \quad \theta(\tau=0) = \theta(\tau=1) = c = \tan^{-1} \left(\frac{\omega_r^2 - |\omega(t)|^2}{2\omega_r \operatorname{Im}(\omega(t))} \right).$$

From (8) we have,

$$Y^I = \operatorname{Tr} \left(\partial_\tau \tilde{U}(\tau) \cdot \tilde{U}(\tau)^{-1} \cdot (M^I)^T \right), \quad (24)$$

where $\operatorname{Tr} (M^I \cdot (M^J)^T) = \delta^{IJ}$. Using this we can define the metric

$$ds^2 = G_{IJ} dY^I dY^{*J}, \quad (25)$$

where the $G_{IJ} = \frac{1}{2} \delta_{IJ}$ is known as a penalty factor. Given the form of $U(s)$ in (21) we will have,

$$ds^2 = d\rho^2 + \cosh(2\rho) \cosh^2 \rho d\mu^2 + \cosh(2\rho) \sinh^2 \rho d\theta^2 - \sinh(2\rho)^2 d\mu d\theta, \quad (26)$$

and the complexity functional defined in (13) will take the form,

$$\mathcal{C}(\tilde{U}) = \int_0^1 d\tau \sqrt{g_{ij} \dot{x}^i \dot{x}^j}. \quad (27)$$

The simplest solution for the geodesic is again a straight line on this geometry [15, 22]. Evaluating (27) we simply get

$$\mathcal{C}(\tilde{U}) = \rho(1) = \frac{1}{2} \left(\cosh^{-1} \left[\frac{\omega_r^2 + |\omega(t)|^2}{2\omega_r \operatorname{Re}(\omega(t))} \right] \right). \quad (28)$$

This is the geodesic distance in the space of $SL(2, R)$ unitaries with end points anchored at the two points determined the boundary conditions (23).

4 Can Circuit Complexity Detect Chaos?

The goal of this paper is to explore whether we can implement the notion of quantum circuit complexity as a diagnostic of a system's chaotic behaviour. Classically, chaos is diagnosed by studying trajectories in the phase space of some dynamical system., a notion that is not well defined in quantum systems, essentially because of the uncertainty principle. It is important to keep in mind then that when we speak of geodesics in the context of circuit complexity, we will mean trajectories defined on the space of unitaries.

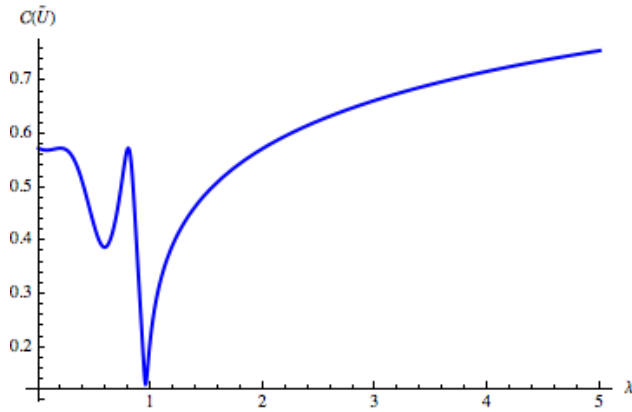


Figure 1: Complexity $\mathcal{C}(\tilde{U})$ vs λ for $t = 7$

As a first step towards realising our goal, let us consider a quantum circuit responsible for producing the state (4) from (2). We will then compute the complexity (geodesic distance) of the target state (4) with respect to (2). It is evident from (5) and (28) that this complexity depends both on time and coupling λ (defined in (1)). First we will study how this complexity changes with coupling λ for a fixed time.

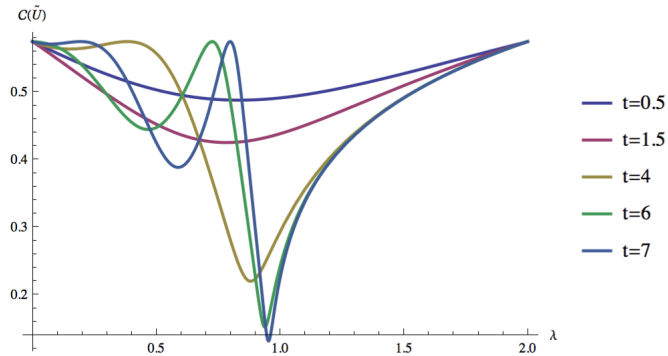


Figure 2: Complexity vs λ for different time. As t increases the other line is forming a cusp. It seems the cusp is formed near $t = 6$.

Interestingly, this displays a cusp-like singular behaviour. The cusp appears at the critical value of $\lambda = \lambda_c$, where the frequency vanishes. Note that the system behaves like a regular oscillator for

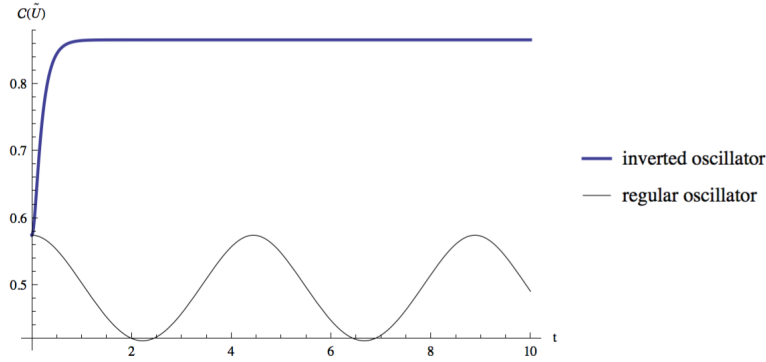


Figure 3: Complexity vs time

$\lambda < \lambda_c$ and an inverted oscillator for $\lambda > \lambda_c$. Since the inverted regime is unstable, it is natural to expect that the complexity will increase with the increase of the coupling, as we would expect the circuit complexity for an inverted oscillator will be large. This is precisely what we see in Fig. 1, on top of the appearance of the cusp, the behaviour of complexity before and after λ_c are completely different, as expected. After the critical value λ_c , when the system enters into the unstable/chaotic regime, complexity grows rapidly with any further increase of the coupling λ .

To our surprise, complexity shows this cusp-like singular behaviour **only** after a certain time t_c . Within this time scale, i.e. for $t < t_c$, the complexity behaves as a continuous function of coupling λ with nothing special going on at $\lambda = \lambda_c$. But as we approach $t = t_c$, the cusp starts to form. To demonstrate this, in Fig. 2, we explore complexities for a set of gradually increasing values of time. For a particular choice of the parameter m , we can see that near $t = 6$ the cusp starts to form. In other words, it takes a certain amount of time for the system to recognize the switch from regular to inverted oscillator.

Before concluding this section, we explore the time evolution of the complexities for both regular and inverted regimes. The results are displayed in Fig. 3. The complexity for the inverted oscillator saturate very quickly. For the regular oscillator the complexity is oscillatory in nature around some average value. Apart from the differences in their appearance, from this time evolution we cannot make any precise statement for the chaotic nature of the system. In the following section we will consider a different class of target state whose complexity will clearly capture the chaotic behaviour.

5 Quantifying Chaos using Complexity

Now we propose a new diagnostic for chaotic behaviour based on circuit complexity. We consider a target state $|\psi_2\rangle$ obtained by evolving a reference state $|\psi_0\rangle$ forward in time with \hat{H} and then backward in time with $\hat{H} + \delta\hat{H}$,

$$|\psi_2\rangle = e^{i(\hat{H}+\delta\hat{H})t}e^{-i\hat{H}t}|\psi_0\rangle. \quad (29)$$

We would like to compute the complexity $\hat{C}(\tilde{U})$ of this target state $|\psi_2\rangle$ with respect to the reference state $|\psi_0\rangle$ [22]. For a chaotic quantum system, even if the two Hamiltonians \hat{H} and $\hat{H} + \delta\hat{H}$ are

arbitrarily close, $|\psi_2\rangle$ will be quite different from $|\psi_0\rangle$.

Having done all the heavy lift already, from (28) we find [22]

$$\hat{\mathcal{C}}(\tilde{U}) = \frac{1}{2} \left(\cosh^{-1} \left[\frac{\omega_r^2 + |\hat{\omega}(t)|^2}{2\omega_r \text{Re}(\hat{\omega}(t))} \right] \right), \quad (30)$$

where now

$$\psi_2(x, t) = \hat{\mathcal{N}}(t) \exp \left[-\frac{1}{2} \hat{\omega}(t) x^2 \right], \quad (31)$$

and

$$\hat{\omega}(t) = i \Omega' \cot(\Omega' t) + \frac{\Omega'^2}{\sin^2(\Omega' t)(\omega(t) + i \Omega' \cot(\Omega' t))}. \quad (32)$$

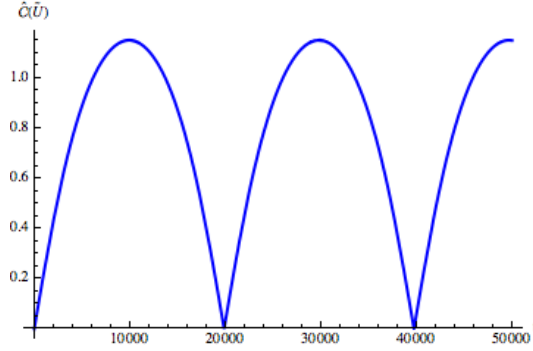


Figure 4: $\hat{\mathcal{C}}(\tilde{U})$ vs time for Regular Oscillator ($m = 1, \lambda = 1.2, \delta\lambda = 0.01$)

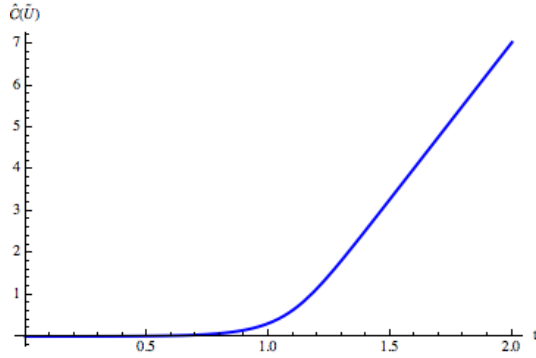


Figure 5: $\hat{\mathcal{C}}(\tilde{U})$ vs time for Inverted Oscillator ($m = 1, \lambda = 15, \delta\lambda = 0.01$)

In this last expression, $\Omega' = \sqrt{m^2 - \lambda'}$ is the frequency associated with the Hamiltonian $H' = \frac{1}{2}p^2 + \frac{\Omega'^2}{2}x^2$ and $\lambda' = \lambda + \delta\lambda$ with $\delta\lambda$ very small. The time dependence of this complexity demonstrates that there is a clear qualitative difference between a regular oscillator and an inverted oscillator as evident from Fig. 4 and Fig. 5. For the regular oscillator we get oscillatory behaviour [22, 23, 24]; the complexity grows linearly for a very short period and reach to a saturation with some fluctuations. However, $\hat{\mathcal{C}}(\tilde{U})$ for the inverted oscillator tells a completely different story.

The overall behaviour of $\hat{\mathcal{C}}(\tilde{U})$ for the inverted oscillator appears to be some complicated monotonically growing function. However, a closer look at Fig. 5, reveals that it takes a small amount of time for the complexity to pick up after which it displays a linear ramp with time. For a different choice of coupling ($\lambda > \lambda_c$) we get similar behaviour with different pick up time and slope (ϕ) for the linear ramp. These features are displayed for different values of the coupling in Fig. 6.

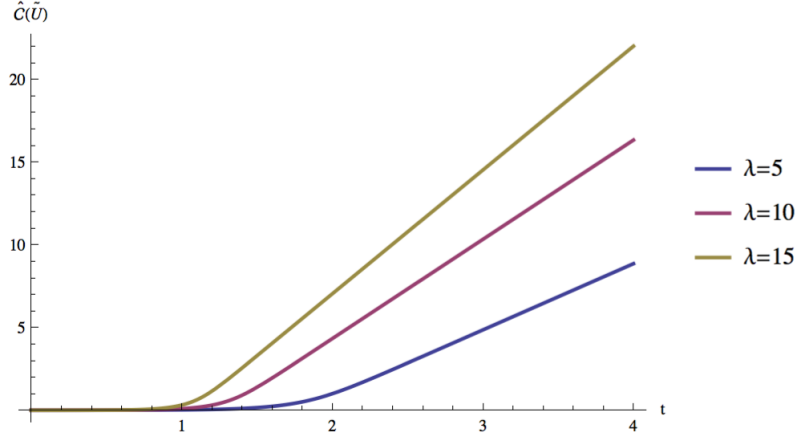


Figure 6: $\hat{\mathcal{C}}(\tilde{U})$ vs time for different values of λ (with $\delta\lambda = 0.01, m = 1$)

As we increase λ (beyond the critical value), we are in effect making the model more unstable and consequently from our very specific circuit model we expect a larger complexity and a smaller pick up time. Therefore, the slope and pick up time scale are natural candidates for measuring the unstable nature of the inverted oscillator. When we explore the slope ϕ of the linear region (as in Fig. 6) for different values of coupling λ we find the behaviour shown in Fig. 7. In the following section, we will argue that this slope is similar to the Lyapunov exponent.

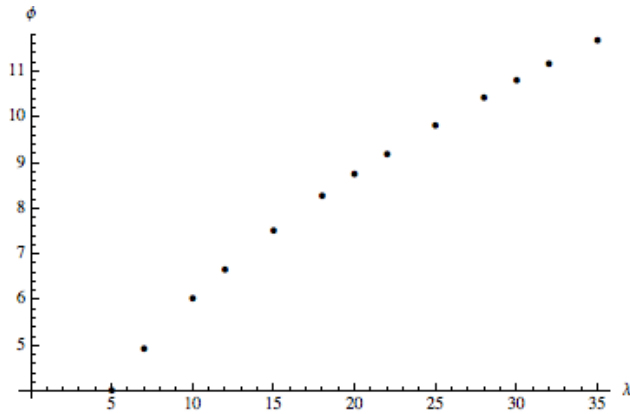


Figure 7: slope ϕ vs λ ($\delta = 0.01, m = 1$)

Note that the linear growth kicks in near a certain time $t = t_s$ (as in the Fig. 5) which depends on the choice of the parameters, $\{m, \lambda\}$. We plot this pick up time as function of λ in Fig. 8. We

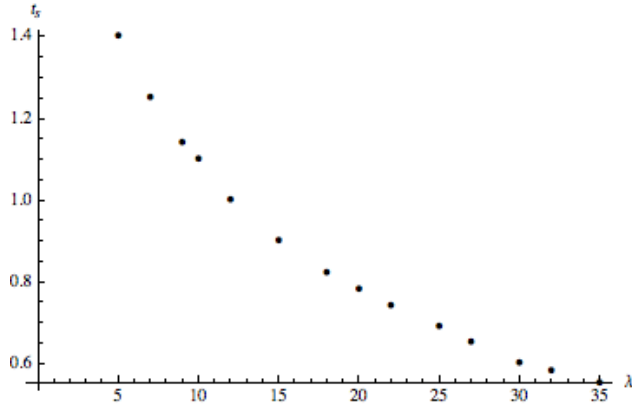


Figure 8: t_s vs λ ($\delta = 0.01, m = 1$)

believe that this time scale is equivalent to the scrambling time which frequently appears in the chaos literature. One way to confirm this is to compute the out-of-time-order four point correlator (OTOC). The time when $\text{OTOC} \sim e^{\Lambda(t-t_*)}$ becomes $\mathcal{O}(1)$, is called the scrambling time. For this oscillator model (1), we can show it analytically following [44]. It is shown in the next section.

We further check the sensitivity of our results to the magnitude of $\delta\lambda$. We plot the $\hat{\mathcal{C}}(\tilde{U})$ for the inverted oscillator for a fixed value of λ but for different $\delta\lambda$. We find that while the slope of the linear region remains same, the pick up time is sensitive to $\delta\lambda$ as exhibited in Fig. 9. We will

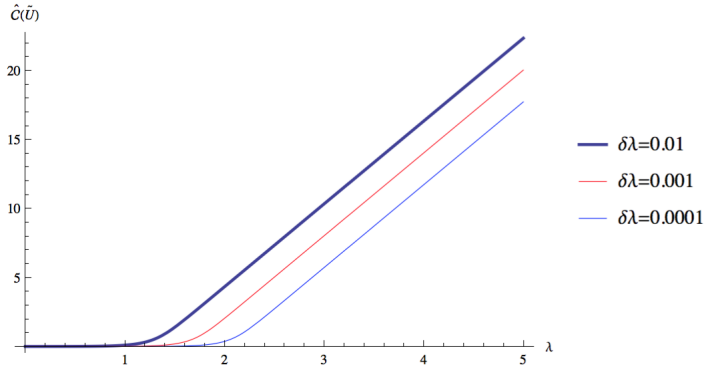


Figure 9: Dependence of $\hat{\mathcal{C}}(\tilde{U})$ on $\delta\lambda$ ($m = 1, \lambda = 10$)

conclude this section by highlighting the fact that we get the same result regarding diagnosing chaos when we explore the circuit complexity (by correlation matrix method), where both target and reference states are evolved by slightly different Hamiltonians from some other state. The equality between these two complexities was concretely shown in [22].

6 OTOC, Lyapunov Exponent and Scrambling Time

The exponential behaviour of the 4-point OTOC has recently emerged as a popular early-time diagnostic for quantum chaos⁸. In [44] the authors demonstrate explicit calculations of OTOCs for harmonic oscillator. For our model, the OTOC for x and p operators (after reinstating the factor of \hbar) gives [44]

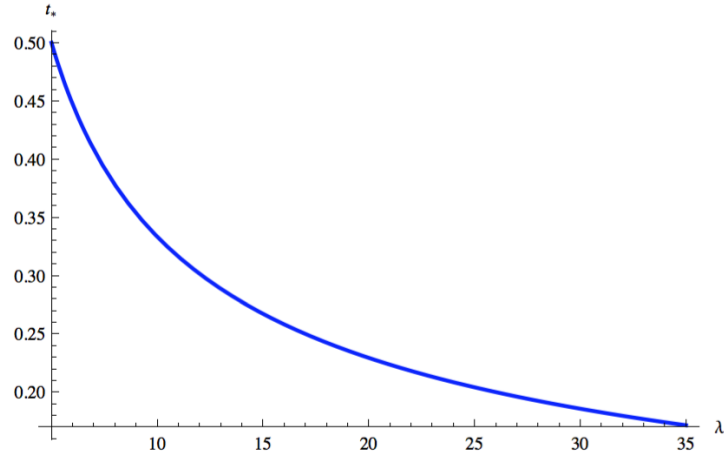


Figure 10: t_* vs λ ($m=1$).

$$\langle [x(t), p]^2 \rangle = \hbar^2 \cos^2 \Omega t, \quad (33)$$

where Ω is defined (1). When Ω is imaginary, we can write the above expression as an exponential function

$$\langle [x(t), p]^2 \rangle \approx \hbar^2 e^{2|\Omega|t} + \dots. \quad (34)$$

Rewriting the above expression as $e^{2\lambda_L(t-t_*)}$, with Lyapunov exponent λ_L allows us to immediately read off that for our system, $\lambda_L = |\Omega|$ while the scrambling (or Ehrenfest) time is given by $t_* = \frac{1}{\lambda_L} \log \frac{1}{\hbar}$. The λ dependence of this time scale (in the units of $\log \frac{1}{\hbar}$) is shown in Fig. 10. The nature of the graph is in agreement with Fig. 8. In fact from Fig. 10 after doing a data-fitting we get for the pick-up time,

$$t_s = \frac{4 \log(2)}{|\Omega|}. \quad (35)$$

In the units of $\log \frac{1}{\hbar}$ this is related to scrambling time t_* as,

$$t_s = 4 \log(2) t_*. \quad (36)$$

Also, the λ dependence of the Lyapunov exponent is shown in Fig. 11. Again the nature of the graph is in agreement with Fig. 7. After fitting the data we get for the slope ϕ of the linear region of the graph in Fig. 7,

$$\phi = 2|\Omega| = 2\lambda_L. \quad (37)$$

⁸An alternative to the OTOC, $F(t) = \langle A^\dagger(t) B^\dagger(0) A(t) B(0) \rangle$, is the thermally averaged commutator-squared $C(t) = \langle [A(t), B(0)]^2 \rangle$ with the two being related through $C(t) = 2 - 2\text{Re}(F(t))$. Unless there is an explicit ambiguity, we will refer to them both as the OTOC.

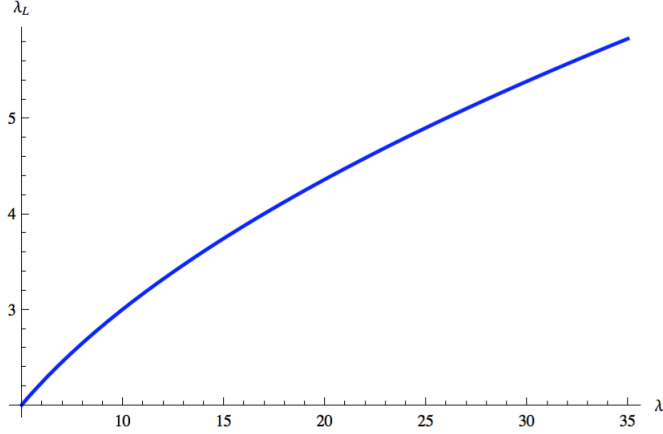


Figure 11: λ_L vs λ ($m=1$).

We have also checked the m -dependence of the slope ϕ and the pick up time t_s and they are in agreement with the m -dependence of λ_L and t_* respectively.

7 Towards a Field Theory Analysis

By using the single oscillator model we have illustrated how complexity can capture chaotic behaviour. In this section we will explore a possible field theory model in which the inverted oscillator appears naturally. Consider two free scalar field theories ((1+1)-dimensional $c = 1$ conformal field theories) deformed by a marginal coupling. The Hamiltonian is given by

$$H = H_0 + H_I = \frac{1}{2} \int dx \left[\Pi_1^2 + (\partial_x \phi_1)^2 + \Pi_2^2 + (\partial_x \phi_2)^2 + m^2(\phi_1^2 + \phi_2^2) \right] + \lambda \int dx (\partial_x \phi_1)(\partial_x \phi_2). \quad (38)$$

We can discretize this theory by putting it on a lattice. Then using the following definitions

$$x(\vec{n}) = \delta \phi(\vec{n}), \quad p(\vec{n}) = \Pi(\vec{n})/\delta, \quad \omega = m, \quad \Omega = \frac{1}{\delta^2}, \quad \hat{\lambda} = \lambda \delta^{-4} \quad \text{and} \quad \hat{m} = \frac{m}{\delta}, \quad (39)$$

we get

$$H = \frac{\delta}{2} \sum_n \left[p_{1,n}^2 + p_{2,n}^2 + \left(\Omega^2 (x_{1,n+1} - x_{1,n})^2 + \Omega^2 (x_{2,n+1} - x_{2,n})^2 + \right. \right. \\ \left. \left. (\hat{m}^2 (x_{1,n}^2 + x_{2,n}^2) + \hat{\lambda} (x_{1,n+1} - x_{1,n})(x_{2,n+1} - x_{2,n})) \right) \right]. \quad (40)$$

Next we perform a series of transformations,

$$x_{1,a} = \frac{1}{\sqrt{N}} \sum_{k=0}^{N-1} \exp\left(\frac{2\pi i k}{N} a\right) \tilde{x}_{1,k}, \\ p_{1,a} = \frac{1}{\sqrt{N}} \sum_{k=0}^{N-1} \exp\left(-\frac{2\pi i k}{N} a\right) \tilde{p}_{1,k},$$

$$\begin{aligned}
x_{2,a} &= \frac{1}{\sqrt{N}} \sum_{k=0}^{N-1} \exp\left(\frac{2\pi i k}{N} a\right) \tilde{x}_{2,k}, \\
p_{2,a} &= \frac{1}{\sqrt{N}} \sum_{k=0}^{N-1} \exp\left(-\frac{2\pi i k}{N} a\right) \tilde{p}_{2,k}, \\
\tilde{p}_{1,k} &= \frac{p_{s,k} + p_{a,k}}{\sqrt{2}}, \quad \tilde{p}_{2,k} = \frac{p_{s,k} - p_{a,k}}{\sqrt{2}}, \\
\tilde{x}_{1,k} &= \frac{x_{s,k} + x_{a,k}}{\sqrt{2}}, \quad \tilde{x}_{2,k} = \frac{x_{s,k} - x_{a,k}}{\sqrt{2}},
\end{aligned} \tag{41}$$

that lead to the Hamiltonian

$$H = \frac{\delta}{2} \sum_{k=0}^{N-1} \left[p_{s,k}^2 + \bar{\Omega}_k^2 x_{s,k}^2 + p_{a,k}^2 + \Omega_k^2 x_{a,k}^2 \right], \tag{42}$$

where

$$\bar{\Omega}_k^2 = \left(\hat{m}^2 + 4(\Omega^2 + \hat{\lambda}) \sin^2\left(\frac{\pi k}{N}\right) \right), \quad \Omega_k^2 = \left(\hat{m}^2 + 4(\Omega^2 - \hat{\lambda}) \sin^2\left(\frac{\pi k}{N}\right) \right). \tag{43}$$

It is immediately clear that by tuning the value of $\hat{\lambda}$, the frequencies Ω_k can be made arbitrarily

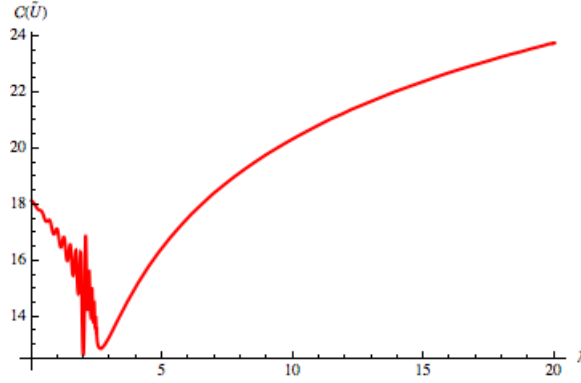


Figure 12: $\mathcal{C}(\tilde{U})$ vs λ for $\delta = 0.1, m = 1, t = 20, N = 1000$.

negative resulting in coupled inverted oscillators. Note that $\bar{\Omega}_k$ will be always positive. Therefore, one can view (42) as a sum of regular and inverted oscillator for each value of k . Now to study the unstable behaviour, the regular oscillator part is not very interesting. Hence, we will simply investigate the inverted oscillator part with the Hamiltonian

$$\tilde{H}(m, \Omega, \hat{\lambda}) = \frac{\delta}{2} \sum_{k=0}^{N-1} \left[p_k^2 + \left(\hat{m}^2 + 4(\Omega^2 - \hat{\lambda}) \sin^2\left(\frac{\pi k}{N}\right) \right) x_k^2 \right]. \tag{44}$$

Note that by tuning $\hat{\lambda}$ for this Hamiltonian one can get both regular and inverted oscillators. Now we want to time evolve with the above Hamiltonian. Specifically, at $t = 0$ we start with the ground state of $\tilde{H}(m, \Omega, \hat{\lambda} = 0)$ and then time evolve it with $\tilde{H}(m, \Omega, \hat{\lambda} \neq 0)$. The complexity for this time evolved target state with respect to the ground state of $\tilde{H}(m, \Omega, \hat{\lambda} = 0)$ is given by a suitable generalization of (28)

$$\mathcal{C}(\tilde{U}) = \frac{1}{2} \sqrt{\sum_{k=0}^{N-1} \left(\cosh^{-1} \left[\frac{\omega_{r,k}^2 + |\omega_k(t)|^2}{2\omega_{r,k} \operatorname{Re}(\omega_k(t))} \right] \right)^2}, \tag{45}$$

where

$$\omega_k(t) = \Omega_k \left(\frac{\Omega_k - i \omega_{r,k} \cot(\Omega_k t)}{\omega_{r,k} - i \Omega_k \cot(\Omega_k t)} \right), \quad (46)$$

and

$$\omega_{r,k}^2 = \hat{m}^2 + 4 \Omega^2 \sin^2 \left(\frac{\pi k}{N} \right). \quad (47)$$

We can also compute $\hat{\mathcal{C}}(\tilde{U})$ as before by considering two Hamiltonians \tilde{H} and \tilde{H}' with two slightly different couplings, $\hat{\lambda}$ and $\hat{\lambda}' = \hat{\lambda} + \delta\hat{\lambda}$, where $\delta\hat{\lambda}$ is small. In this case we get

$$\hat{\mathcal{C}}(\tilde{U}) = \frac{1}{2} \sqrt{\sum_{k=0}^{N-1} \left(\cosh^{-1} \left[\frac{\omega_{r,k}^2 + |\hat{\omega}_k(t)|^2}{2 \omega_{r,k} \operatorname{Re}(\hat{\omega}_k(t))} \right] \right)^2}, \quad (48)$$

where

$$\hat{\omega}_k(t) = i \Omega'_k \cot(\Omega'_k t) + \frac{\Omega_k'^2}{\sin^2(\Omega'_k t) (\omega_k(t) + i \Omega'_k \cot(\Omega'_k t))}, \quad \Omega_k'^2 = \hat{m}^2 + 4 (\Omega^2 - \hat{\lambda} - \delta\hat{\lambda}) \sin^2 \left(\frac{\pi k}{N} \right) \quad (49)$$

and $\omega_k(t)^2$, $\omega_{r,k}^2$ are defined in (46).

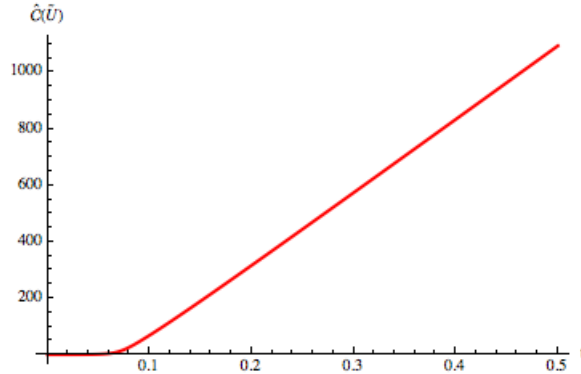


Figure 13: $\hat{\mathcal{C}}(\tilde{U})$ vs time for the Inverted Oscillators ($\delta = 0.1, m = 1, N = 1000, \hat{\lambda}\delta^2 = 10, \delta\hat{\lambda} = 0.01$)

Now we compute the complexity. Just as in the single oscillator case, we observe the formation of a cusp as the system switches from regular to inverted oscillator. Fig. 12 shows the appearance of cusp. Moreover, we confirmed that the cusp starts to appear at a certain time scale. Also, using our testing method (outlined in section 5), once again for the inverted oscillator we can immediately read off the scrambling time and Lyapunov exponent from the time evolution of $\hat{\mathcal{C}}(\tilde{U})$ as shown in from Fig. 13.

8 Discussion

In this paper we used a harmonic oscillator model that converts to an inverted oscillator for large coupling of the interaction Hamiltonian. The coupling behaves as a regulator and by tuning it we can switch between regular and inverted regimes. Our motivation was to use this inverted oscillator

as a toy model to study quantum chaos. In this context, the regular oscillator serves as a reference system. We developed a new diagnostic for quantum chaos by constructing a particular quantum circuit and computing the corresponding complexity. Our diagnostic can extract equivalent information as the out-of-time-order correlator with the additional feature that complexity can detect when the system switches from regular to the chaotic regime.

By considering the target state as a time evolved state and investigating how complexity changes with coupling, we find a new time scale, which we call the *onset time*. The onset time tells us how long it takes for the system to recognize the transition from regular to unstable regime. Then we considered a target state which is first forward evolved and then backward evolved with slightly different Hamiltonians and found that the behaviour for the regular and inverted oscillator are completely different in this case. For the regular oscillator we get some oscillatory behaviour as in [21, 22, 24]. However, for the inverted oscillator we get an exponential type function with two distinct features: for an initial period the complexity is nearly zero, after which it exhibits a steep linear growth. By comparing with the operator product expansion, we discovered the small time scale and slope of the linear portion to be equivalent to the scrambling time and the Lyapunov exponent respectively.

To give a proof-of-principle argument for complexity as a chaos diagnostic, we have used the inverted oscillator as a toy model. This is, however, a rather special example and, by no means, a realistic chaotic system. To put complexity on the same footing as, say the OTOC as a probe of quantum chaos will take much more work, with more ‘realistic’ systems like the maximally-chaotic SYK model⁹ and its many variants (see, for example, [46, 47, 48] and references therein) in the (0+1)-dimensional quantum mechanical context, or the MSW class of (1+1)-dimensional (non-maximally) chaotic conformal field theories [49].

As a final point of motivation, we note that by virtue of the recent ‘complexity=action’ [50] and ‘complexity=volume’ [51] conjectures, the computational complexity of holographic quantum system has a well-defined (if not entirely unambiguous) dual. This opens up tantalising new possibilities in the study of quantum chaos in strongly coupled quantum systems. We leave these issues for future work.

Acknowledgements

We would like to thank Dario Rosa and Jon Shock for useful comments. AB thanks Aninda Sinha, Pratik Nandy, Jose Juan Fernandez-Melgarejo and Javier Molina Vilaplana for many discussions and ongoing collaborations on complexity. AB also thanks Department of Physics, University of Windsor, Perimeter Institute and FISPAC group (specially Jose Juan Fernandez-Melgarejo and E. Torrente-Lujan) of Department of Physics, University of Murcia for their warm hospitality during this work. AB is supported by JSPS Grant-in-Aid for JSPS fellows (17F17023). JM is supported by the NRF of South Africa under grant CSUR 114599. NM is supported by the South African

⁹It is worth pointing out that as this manuscript was being prepared, we were made aware of the recent article [45] also advocating for the idea of complexity as a tool for the study of quantum chaotic systems.

Research Chairs Initiative of the Department of Science and Technology and the National Research Foundation of South Africa. Any opinion, finding and conclusion or recommendation expressed in this material is that of the authors and the NRF does not accept any liability in this regard. Research at Perimeter Institute is supported by the Government of Canada through the Department of Innovation, Science, and Economic Development, and by the Province of Ontario through the Ministry of Research and Innovation.

References

- [1] Interested readers are referred to the following thesis and the references therein.
N. Hunter-Jones, “Chaos and Randomness in Strongly-Interacting Quantum Systems”, PhD thesis, California Institute of Technology, 2018, <https://thesis.library.caltech.edu/11002/>,
- [2] F. Haake, “Quantum Signatures of Chaos,” Springer, 2010.
- [3] A. Peres, *Quantum theory: concepts and methods*, Vol. 72 of *Fundamental theories of physics* (Kluwer, Dordrecht, 1995).
- [4] R. A. Jalabert and H. M. Pastawski, *Environment-independent decoherence rate in classically chaotic systems*, Phys. Rev. Lett. **86**, 2490 (2001).
- [5] O. Bohigas, M. J. Giannoni, and C. Schmit, “Characterization of Chaotic Quantum Spectra and Universality of Level Fluctuation Laws,” Phys. Rev. Lett. 52 (1984) 1.
- [6] S. H. Shenker and D. Stanford, “Black holes and the butterfly effect,” JHEP 03 (2014) 067, arXiv:1306.0622 [hep-th].
- [7] S. H. Shenker and D. Stanford, “Stringy effects in scrambling,” JHEP 05 (2015) 132, arXiv:1412.6087 [hep-th].
- [8] A. Kitaev, “A simple model of quantum holography.” Talks given at the KITP, Apr. 7, 2015 and May 27, 2015.
- [9] J. Maldacena, S. H. Shenker, and D. Stanford, “A bound on chaos,” JHEP 08 (2016) 106, arXiv:1503.01409 [hep-th].
- [10] A. I. Larkin and Y. N. Ovchinnikov, “Quasiclassical Method in the Theory of Superconductivity,” JETP 28 (1969) 1200.
- [11] P. Hayden and J. Preskill, “Black holes as mirrors: Quantum information in random subsystems,” JHEP 09 (2007) 120, arXiv:0708.4025 [hep-th].
- [12] Y. Sekino and L. Susskind, “Fast Scramblers,” JHEP 10 (2008) 065, arXiv:0808.2096 [hep-th].
- [13] N. Lashkari, D. Stanford, M. Hastings, T. Osborne, and P. Hayden, “Towards the Fast Scrambling Conjecture,” JHEP 04 (2013) 022, arXiv:1111.6580 [hep-th].
- [14] T. Nosaka, D. Rosa and J. Yoon, JHEP **1809**, 041 (2018) doi:10.1007/JHEP09(2018)041 [arXiv:1804.09934 [hep-th]].

- [15] R. A. Jefferson and R. C. Myers, *Circuit complexity in quantum field theory*, *JHEP* **10** (2017) 107, [arXiv:1707.08570[hep-th]].
- [16] M. Guo, J. Hernandez, R. C. Myers and S. M. Ruan, “*Circuit Complexity for Coherent States*,” arXiv:1807.07677 [hep-th].
- [17] L. Hackl and R. C. Myers, “*Circuit complexity for free fermions*,” arXiv:1803.10638 [hep-th]
- [18] R. Khan, C. Krishnan, and S. Sharma, *Circuit Complexity in Fermionic Field Theory*, [arXiv:1801.07620[hep-th]].
- [19] S. Chapman, M. P. Heller, H. Marrochio and F. Pastawski, “*Toward a Definition of Complexity for Quantum Field Theory States*,” *Phys. Rev. Lett.* **120** (2018) no.12, 121602 [arXiv:1707.08582 [hep-th]],
- [20] H. A. Camargo, P. Caputa, D. Das, M. P. Heller and R. Jefferson, “*Complexity as a novel probe of quantum quenches: universal scalings and purifications*,” arXiv:1807.07075 [hep-th],
- [21] A. Bhattacharyya, A. Shekar and A. Sinha, “*Circuit complexity in interacting QFTs and RG flows*,” *JHEP* **1810** (2018) 140 doi:10.1007/JHEP10(2018)140 [arXiv:1808.03105 [hep-th]].
- [22] T. Ali, A. Bhattacharyya, S. Shajidul Haque, E. H. Kim and N. Moynihan, “*Time Evolution of Complexity: A Critique of Three Methods*,” *JHEP* **1904** (2019) 087 [arXiv:1810.02734 [hep-th]].
- [23] T. Ali, A. Bhattacharyya, S. Shajidul Haque, E. H. Kim and N. Moynihan, “*Post-Quench Evolution of Distance and Uncertainty in a Topological System: Complexity, Entanglement and Revivals*,” arXiv:1811.05985 [hep-th].
- [24] S. Chapman, J. Eisert, L. Hackl, M. P. Heller, R. Jefferson, H. Marrochio and R. C. Myers, “*Complexity and entanglement for thermofield double states*,” *SciPost Phys.* **6** (2019) no.3, 034 [arXiv:1810.05151 [hep-th]],
- [25] K. Hashimoto, N. Iizuka, and S. Sugishita, *Time Evolution of Complexity in Abelian Gauge Theories - And Playing Quantum Othello Game*, [arXiv:1707.03840[hep-th]], R.-Q. Yang, *A Complexity for Quantum Field Theory States and Application in Thermofield Double States*, [arXiv:1709.00921[hep-th]], R.-Q. Yang, C. Niu, C.-Y. Zhang, and K.-Y. Kim, *Comparison of holographic and field theoretic complexities for time dependent thermofield double states*, *JHEP* **02** (2018) 082, [arXiv:1710.00600 [hep-th]], D. W. F. Alves and G. Camilo, “*Evolution of Complexity following a quantum quench in free field theory*,” arXiv:1804.00107 [hep-th], J. Jiang, J. Shan and J. Yang, “*Circuit complexity for free Fermion with a mass quench*,” arXiv:1810.00537 [hep-th], R. Q. Yang and K. Y. Kim, *JHEP* **1903** (2019) 010 [arXiv:1810.09405 [hep-th]], S. Liu, “*Complexity and scaling in quantum quench in 1 + 1 dimensional fermionic field theories*,” arXiv:1902.02945 [hep-th],
- [26] P. Caputa, N. Kundu, M. Miyaji, T. Takayanagi and K. Watanabe, “*Anti-de Sitter Space from Optimization of Path Integrals in Conformal Field Theories*,” *Phys. Rev. Lett.* **119** (2017) no.7, 071602 [arXiv:1703.00456 [hep-th]], P. Caputa, N. Kundu, M. Miyaji, T. Takayanagi and K. Watanabe, “*Liouville Action as Path-Integral Complexity: From Continuous Tensor Networks*

- to *AdS/CFT*,” JHEP **1711** (2017) 097 [arXiv:1706.07056 [hep-th]], B. Czech, “*Einstein Equations from Varying Complexity*,” Phys. Rev. Lett. **120** (2018) no.3, 031601 [arXiv:1706.00965 [hep-th]], J. Molina-Vilaplana and A. Del Campo, “*Complexity Functionals and Complexity Growth Limits in Continuous MERA Circuits*,” arXiv:1803.02356 [hep-th], A. Bhattacharyya, P. Caputa, S. R. Das, N. Kundu, M. Miyaji and T. Takayanagi, “*Path-Integral Complexity for Perturbed CFTs*,” JHEP **1807** (2018) 086 [arXiv:1804.01999 [hep-th]], T. Takayanagi, “*Holographic Spacetimes as Quantum Circuits of Path-Integrations*,” arXiv:1808.09072 [hep-th], H. A. Camargo, M. P. Heller, R. Jefferson and J. Knaute, “Path integral optimization as circuit complexity,” arXiv:1904.02713 [hep-th].
- [27] R. Q. Yang, Y. S. An, C. Niu, C. Y. Zhang and K. Y. Kim, “*Axiomatic complexity in quantum field theory and its applications*,” arXiv:1803.01797 [hep-th], P. Caputa and J. M. Magan, “*Quantum Computation as Gravity*,” arXiv:1807.04422 [hep-th], R. Q. Yang, Y. S. An, C. Niu, C. Y. Zhang and K. Y. Kim, “*More on complexity of operators in quantum field theory*,” arXiv:1809.06678 [hep-th], A. Bernamonti, F. Galli, J. Hernandez, R. C. Myers, S. M. Ruan and J. Simn, “The First Law of Complexity,” arXiv:1903.04511 [hep-th], I. Akal, “Weighting gates in circuit complexity and holography,” arXiv:1903.06156 [hep-th] G. Camilo, D. Melnikov, F. Novaes and A. Prudenziati, “Circuit Complexity of Knot States in Chern-Simons theory,” arXiv:1903.10609 [hep-th] A. R. Brown and L. Susskind, “The Complexity Geometry of a Single Qubit,” arXiv:1903.12621 [hep-th], D. Ge and G. Policastro, “Circuit Complexity and 2D Bosonisation,” arXiv:1904.03003 [hep-th] W. H. Huang, “Operator Approach to Complexity : Excited State,” arXiv:1905.02041 [hep-th], V. Balasubramanian, M. DeCross, A. Kar and O. Parrikar, “Binding Complexity and Multiparty Entanglement,” JHEP **1902** (2019) 069 [arXiv:1811.04085 [hep-th]].
- [28] M. A. Nielsen, *A geometric approach to quantum circuit lower bounds*, [arXiv:quant-ph/0502070].
- [29] M. A. Nielsen, M. R. Dowling, M. Gu, and A. M. Doherty, *Quantum Computation as Geometry*, *Science* **311** (2006) 1133–1135, [arXiv:quant-ph/0603161].
- [30] M. A. Nielsen and M. R. Dowling, *The geometry of quantum computation*, [arXiv:quant-ph/0701004].
- [31] M. Miyaji, “Butterflies from Information Metric,” JHEP **1609** (2016) 002 doi:10.1007/JHEP09(2016)002 [arXiv:1607.01467 [hep-th]].
- [32] P. Hosur, X.-L. Qi, D. A. Roberts, and B. Yoshida, “Chaos in quantum channels,” JHEP **02** (2016) 004, arXiv:1511.04021 [hep-th].
- [33] D. A. Roberts and B. Yoshida, “Chaos and complexity by design,” JHEP **04** (2017) 121, arXiv:1610.04903 [quant-ph].
- [34] J. Cotler, N. Hunter-Jones, J. Liu, and B. Yoshida, “Chaos, Complexity, and Random Matrices,” JHEP **11** (2017) 048, arXiv:1706.05400 [hep-th].
- [35] J. M. Magan, “*Black holes, complexity and quantum chaos*,” arXiv:1805.05839 [hep-th].

- [36] V. Balasubramanian, M. DeCross, A. Kar and O. Parrikar, “Quantum Complexity of Time Evolution with Chaotic Hamiltonians,” arXiv:1905.05765 [hep-th].
- [37] A. Y. Yosifov and L. G. Filipov, “Quantum Complexity and Chaos in Young Black Holes,” Universe **5** (2019) no.4, 93 [arXiv:1904.09767 [hep-th]].
- [38] G. Barton, *Quantum mechanics of the inverted oscillator*, Ann. Phys. **166**, 322 (1986).
- [39] R. Blume-Kohout and W. Zurek, *Decoherence from a chaotic environment: an upside-down “oscillator” as a model*, Phys. Rev. A **68**, 032104 (2003).
- [40] S. Gentilini, M. C. Braidotti, G. Marcucci, E. DelRe, and C. Conti, *Physical realization of the Glauber quantum oscillator*, Sci. Rep. **5**, 15816 (2015).
- [41] M. V. Berry and J. P. Keating, *The Riemann zeros and eigenvalue asymptotics*, SIAM Rev. **41**, 236 (1999).
- [42] T. Morita, “Thermal Emission from Semi-classical Dynamical Systems,” Phys. Rev. Lett. **122** (2019) no.10, 101603 doi:10.1103/PhysRevLett.122.101603 [arXiv:1902.06940 [hep-th]].
T. Morita, “Semi-classical bound on Lyapunov exponent and acoustic Hawking radiation in $c = 1$ matrix model,” arXiv:1801.00967 [hep-th].
- [43] See, e.g. R. Shankar, *Principles of Quantum Mechanics* (Plenum, New York, 1994).
- [44] K. Hashimoto, K. Murata, and R. Yoshii: *Out-of-time-order correlators in quantum mechanics*, JHEP **10** 138 (2017).
- [45] V. Balasubramanian, M. DeCross, A. Kar and O. Parrikar, “Quantum Complexity of Time Evolution with Chaotic Hamiltonians,” arXiv:1905.05765 [hep-th].
- [46] J. Maldacena and D. Stanford, “Remarks on the Sachdev-Ye-Kitaev model,” Phys. Rev. D **94**, no. 10, 106002 (2016) [arXiv:1604.07818 [hep-th]].
- [47] W. Fu, D. Gaiotto, J. Maldacena and S. Sachdev, “Supersymmetric Sachdev-Ye-Kitaev models,” Phys. Rev. D **95**, no. 2, 026009 (2017) Addendum: [Phys. Rev. D **95**, no. 6, 069904 (2017)] [arXiv:1610.08917 [hep-th]].
- [48] A. Kitaev and S. J. Suh, “The soft mode in the Sachdev-Ye-Kitaev model and its gravity dual,” JHEP **1805**, 183 (2018) [arXiv:1711.08467 [hep-th]].
- [49] J. Murugan, D. Stanford and E. Witten, “More on Supersymmetric and 2d Analogs of the SYK Model,” JHEP **1708**, 146 (2017) [arXiv:1706.05362 [hep-th]].
- [50] A. R. Brown, D. A. Roberts, L. Susskind, B. Swingle and Y. Zhao, “Holographic Complexity Equals Bulk Action?,” Phys. Rev. Lett. **116**, no. 19, 191301 (2016) [arXiv:1509.07876 [hep-th]].
- [51] D. A. Roberts, D. Stanford and L. Susskind, “Localized shocks,” JHEP **1503**, 051 (2015) [arXiv:1409.8180 [hep-th]].